Modeling the Impact of Hydraulic Fracturing of Amber-Bearing Rocks by a Flooded Jet in the Erosion Chamber on Mining Productivity

Valerii KORNIYENKO[1)], Yevhenii MALANCHUK[2)], Vitalii ZAIETS[3)], Mykola KOZIAR[4)], Olexandr VASYLCHUK[5)], Wiktoria SOBCZYK[6)]

[1)] Doctor of Engineering, Professor, Department of Mineral Deposits Development and Mining Engineering, National University of Water and Environmental Engineering, Soborna str, 11, Rivne, Ukraine
[2)] Doctor of Engineering, Professor, Department of Automation, Electrical Engineering and Computer-Integrated Technologies, National University of Water and Environmental Engineering, Soborna str, 11, Rivne, Ukraine
[3)] PhD, Associate Professor, Department of Mineral Deposits Development and Mining Engineering, National University of Water and Environmental Engineering, Soborna str, 11, Rivne, Ukraine; email: v.v.zayets@nuwm.edu.ua
[4)] Doctor of Pedagogical Sciences, Professor, Department of Theoretical Mechanics, Engineering Graphics and Machine Sciences, National University of Water and Environmental Engineering, Soborna str, 11, Rivne, Ukraine
[5)] PhD, Associate Professor, Department of Mineral Deposits Development and Mining Engineering, National University of Water and Environmental Engineering, Soborna str, 11, Rivne, Ukraine
[6)] Prof. DSc, PhD, Eng. Faculty of Energy and Fuels, Dept. of Sustainable Energy Development, AGH University of Science & Technology, Krakow, Poland

http://doi.org/10.29227/IM-2024-01-105

Submission date: 13-05-2024 | Review date: 24-06-2024

Abstract

The article discusses the concept of socio-economic and strategic development of the Rivne region (Ukraine), especially the exploration, testing and industrial exploitation of strategic mineral resources. The concept envisages the use of energy-efficient technologies for raw material extraction, especially for amber deposits. It points out that conventional methods of amber extraction are harmful to the environment, and suggests the use of complex methods, such as mechanical and hydraulic technologies.

The article examines the challenge of implementing geotechnological methods at mining enterprises and assesses its complexity in mining science and practice. Scientific research in this area has been conducted, but comprehensive studies of the sampling and extraction methods of amber are still significant and relevant for the national interest.

Moreover, the article reports the results of research on the formation of a jet in a hydraulic monitor and the application of a telescopic hydraulic monitor to extend the range of rock fragmentation, including an analysis of jet parameters and the dynamics of hydraulic rock breaking, such as amber-bearing rocks. The conclusions relate to the linear expansion of the jet, the reduction of axial velocity with the increase of hydrostatic pressure and the efficiency of the telescopic hydromonitor to extend the fragmentation range.

Keywords: *amber, hydromonitor, submerged jet, destruction, parameters*

Introduction

The article outlines the concept of socio-economic and strategic development of the Rivne region of Ukraine, focusing on the exploration, testing and industrial exploitation of strategic mineral resources, located in the subsoil of this region. The concept proposes the creation and implementation of innovative energy-saving technologies for raw material extraction at various stages of sampling, testing and development of deposits, enhancing their energy efficiency through automation of technological processes, reducing costs, and ensuring environmental sustainability of operating conditions. Among other minerals, the development of amber deposits has been identified as a priority. However, the conventional and widespread open method is harmful to the environment. Analytical review and experience indicate that such technologies should rely on the use of integrated extraction methods that combine both mechanical and hydraulic technologies.

Evaluation of the problem status has revealed that the successful implementation of geotechnological methods at mining enterprises is one of the most promising tasks in this area, but also very challenging in mining science and practice.

To date, scientists have conducted research and achieved scientific results on this problem in the leading schools of mining and related sciences, but comprehensive studies of sampling and extraction methods, technology parameters for a significant improvement in the extraction completeness cannot be applied to amber deposits.

Therefore, the development of theoretical and applied foundations of mechanical-hydraulic technology for testing, trial operation and development of amber deposits is an urgent scientific and practical problem of important national importance.

1. Disintegration of Host Rocks by Hydromonitor Jets

The jet formation in the hydraulic monitor depends on the water flow encountering different supports on its way to the nozzle, which cause turbulization and cavitation of the flow, reducing the quality and parameters of the hydraulic monitor jet. The jet is finally formed in the nozzle, which transforms the static pressure of water into the kinetic energy of the jet, and as the nozzle cross-section decreases with a constant water flow rate, its speed increases. Meanwhile, the head loss in the nozzle increases, which is proportional to the square of

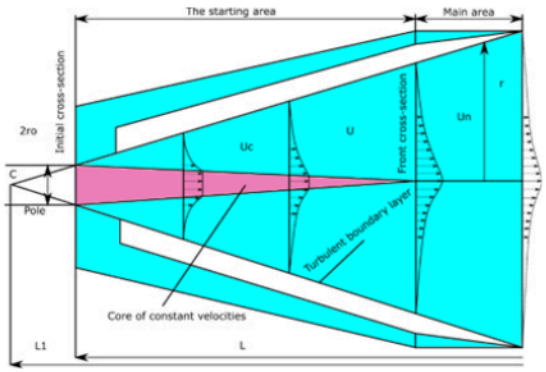

Fig. 1. Diagram of the flooded jet: r0 – nozzle radius; o – pole of jets; uo – initial jet outflow velocity; um – the speed of the jet along its axis; u – velocity of the jet at an arbitrary point along the cross-section; r – current jet radius; l – current jet length; l1 – jet length given pole

Rys. 1. Schemat zalanego strumienia: r0 – promień dyszy; o – słup dysz; uo – początkowa prędkość wypływu strumienia; um – prędkość strumienia wzdłuż jego osi; u – prędkość strumienia w dowolnym punkcie przekroju; r – aktualny promień strumienia; l – aktualna długość strumienia; l1 – długość strumienia na danym biegunie

the flow rate. In the final section of the nozzle, static pressure without head loss is converted into velocity head.

The speed of the jet departure, the water flow rate and the diameter of the hydraulic monitor nozzle are determined by the formulas:

$$u_o = \phi\sqrt{2gH} \tag{1}$$

$$Q = \mu S_H \sqrt{2gH} \tag{2}$$

$$d_н = 0{,}52\sqrt{\frac{Q}{\sqrt{H}}} \tag{3}$$

S_H – cross-sectional area of the nozzle outlet;
H – pressure;
Q – consumption;
φ – speed ratio (φ = 0,92–0,9b);
μ = αφ;
α – jet compression ratio (α≈1).

According to Prandtl's boundary layer theory, the jet dispersion is caused by the turbulent exchange between it and the surrounding fluid, and the viscosity is the reason for the formation of vortices at the interface between the jet and the liquid. These vortices impede the jet motion and increase its mass by drawing in fluid from the outside. Figure 1 illustrates the jet structure common to all types and its main elements.

The jet structure is defined by geometric (length of the initial and main jet sections, expansion angle) and hydraulic (initial flow speed from the nozzle, axial speed and flow speed across the jet cross-section) parameters [1-5].

The structure and initial parameters of the jet match the conditions for the water flow formation in the channels. Turbulence of the water flow in the supply channel, irregularity of the longitudinal speed profile of the jet, turbulence of the water flow at the nozzle entrance, and cavitation at high heads are factors that reduce the jet compactness and, consequently, its effective length. Besides them, the jet parameters are affected by the viscosity and density of the medium where the jet propagates. Hydraulic and geometric parameters determine the most important jet indicators in contact with the rock - impact force and specific dynamic pressure [6-11].

The decay of a free submerged jet is caused by its expansion due to turbulent exchange with the environment under the effect of inertial forces and surface tension [12-16]. In a non-free flooded jet, the same viscous friction forces and medium resistance have a greater role because of its higher density compared to the jet substance density (Figure 2).

The medium density can increase due to its pressure increase, for example, hydrostatic, because of the production deepening. As a result, the hydrodynamic parameters of the flooded jet worsen. This happens during hydraulic sandblasting of oil well bottomhole zones. The results of measuring the dynamic pressure of the jet at different depths are shown in figure 3. The graph shows that hydrostatic pressure up to a depth of 200-300 meters significantly deteriorates the jet parameters. Studies have also revealed that the effect of the medium density increase with the hydrostatic pressure increase is related to the presence of air bubbles in the liquid flowing out through the nozzle.

The hydromonitor jet, when traveling in the air at a certain distance from the nozzle at the end of the initial section, almost falls apart and can be described by a statistical analysis of the individual elements of the moving water-air mixture. The general form of the fluid mechanics equations for turbulent motion of discrete media has no solution.

Some researchers [23-28, 32] have found empirical relationships of jet parameters on the distance to the nozzle for specific conditions.

Hydromonitor jets can virtually break rocks of any hardness. However, jet fracture is mainly used in the development of weakly cohesive and loose rocks (sands, loams, clayey sandstones, siltstones, etc.) and less frequently semi-rocky rocks (coal, mudstones, marls, shales, limestone sandstones, and so on) [33-39].

According to the results of many experimental studies, it has been determined that the destruction mechanism is due to the simultaneous action of various forces and depends on the characteristics of rocks and the conditions of the jet flow [40-43]. With the destruction of weakly cohesive and loose rocks as a result of the pulsating action of the jet, the bond between the individual particles of the erosion rock is broken. As a result of filtration of part of the water into the pores of loose rocks, they are moistened and wetted, which leads to a change in the adhesion force of the particles. In addition, in an unflooded face, the mass of water of the jet, which accumulates in the funnel, bursts it and, as a result, stresses arise

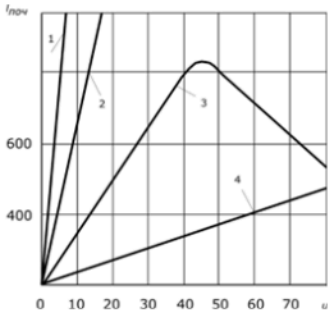

Fig. 2. Change in the length of the initial section of the jet depending on the outflow velocity: 1 – water; 2 – glycerin; 3 – oil: 4 – mercury; l_{init} – length of the initial section of the jet (mm); и – jet speed (m/s)

Rys. 2. Zmiana długości początkowego odcinka strumienia w zależności od prędkości wypływu: 1 – woda; 2 – gliceryna; 3 – olej: 4 – rtęć; $l_{pocz.}$ – długość początkowego odcinka strumienia (mm); u –prędkość strumienia (m/s)

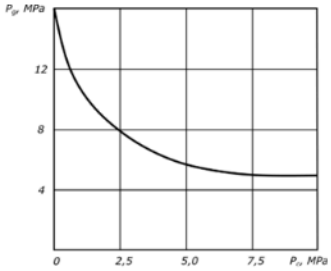

Fig. 3. Dependence of the dynamic head of the jet (P_g) on the hydrostatic pressure (P_c) of the aqueous medium at the pressure at the outlet of the nozzle of 20 MPa

Rys. 3. Zależność wysokości dynamicznej strumienia (P_g) od ciśnienia hydrostatycznego (P_c) ośrodka wodnego przy ciśnieniu na wylocie dyszy, wynoszącym 20 MPa

in the massif, contributing to the emergence of cracks and the detachment of individual pieces of rock.

The shear resistance of cohesive soils is expressed by Coulomb's formula

$$\tau = c + \sigma_e tg\ \varphi \quad (4)$$

σ_e – effective normal voltage;
τ – shear stress;
φ – angle of internal friction;
c – specific adhesion.

For cemented sands and similar rocks

$$\tau = c + (\sigma - p_\Gamma) tg\ \varphi \quad (5)$$

σ – full normal voltage;
p_Γ – neutral voltage equal to the hydrostatic pressure of water in the pores. For loose sands, you can take the specific adhesion to be zero.

To break weakly cohesive and loose rocks, the jet pressure at the contact must exceed the shear resistance [45-48].

The structure of the massif can be destroyed by creating a hydraulic gradient for very loose water-saturated soils and quicksand, which have a specific ratio of fractions and a degree of water saturation.

Investigation of hydrodynamic characteristics of the jet in mechanical-hydraulic extraction of amber. The study involved measuring the dynamic pressure of the flooded jet along its axis and across its cross-section at various distances from the nozzle depending on the nozzle diameters, water pressure, and the effect of the hydrostatic pressure of the amber deposit on the jet parameters.

To conduct field studies on the exposed layer of the Klesiv amber deposit in the Rivne region, a bench installation was built (Figure 4). A layer with a thickness of 3 meters from top to bottom consists of different-, medium- and fine-grained host rock, the strength of which is characterized by an adhesion coefficient of 0.03, 0.035 and 0.045 MPa. The telescopic barrel is placed at a distance from the face and closed with a jet cut-off to avoid erosion when measuring the fixed water pressure on the nozzle. Before the experiment, the pit was filled with water to a depth of more than 1 meter. In the course of the experiment, the time of operation of the jet and the pressure of water on the nozzle were fixed. After the experiment, the hydraulic mixture was pumped out of the chamber by a hydraulic elevator, and the formed cavity was measured [50, 53-54, 56, 58].

The bench installation enabled the experiment conditions to be as close as possible to the full-scale ones, to vary the pressure of the pressure water in front of the nozzle in a wide range and to measure the dynamic pressure of the jet along the axis and in its different sections.

It is well known that destructive processes are quite hard to model with physical similarity. It will be shown later that even a more stable process of mineral transportation is quite hard to model.

The dynamic pressure was measured by a receiving nozzle, which moved in three mutually perpendicular planes with the help of a system of adjusting bolts. The experiment started with mounting, centering and securing the nozzle and breaker plate. Then, a container measuring 2.5×1.5×1.5 m was filled with water, air was released from the impulse

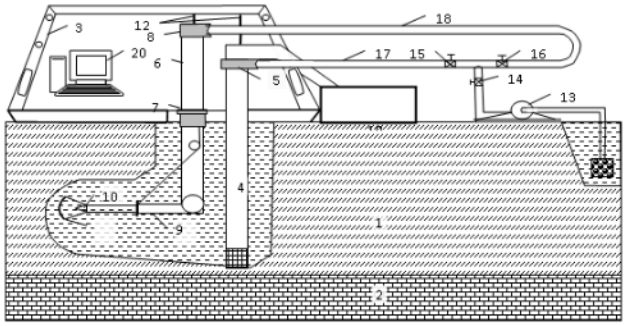

Fig. 4. Stand for field studies of hydraulic destruction of minerals in a flooded environment: 1 –mineral, 2 – underlying rocks; 3 – assembly crane; 4 – hydroelevator, 5 – hydraulic elevator header; 6 – hydromonitor device, 7 – rotator, 8 – headband, 9 – technological barrel, 10 – nozzle, 11 – jet cut-off, 12 – cable block system, 13 – pump, 14-16 – latches, 17, 18 – flexible high-pressure hoses, 19 – container for hydraulic mixture, 20 – control panel

Rys. 4. Stanowisko do badań terenowych hydraulicznego niszczenia minerałów w środowisku zalewowym: 1 – minerał, 2 – skały leżące pod spodem; 3 – dźwig montażowy; 4 – winda hydrauliczna, 5 – głowica windy hydraulicznej; 6 – urządzenie hydromonitorowe, 7 – rotator, 8 – opaska nagłowna, 9 – beczka technologiczna, 10 – dysza, 11 – odcięcie strumienia, 12 – układ bloków kablowych, 13 – pompa, 14-16 – zatrzaski, 17, 18 – elastyczne węże wysokociśnieniowe, 19 – zbiornik na mieszankę hydrauliczną, 20 – panel sterowania

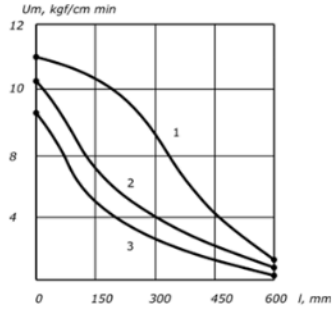

Fig. 5. Distribution of axial velocity (U_m) along the length of the flooded jet (l) for conoidal-cylindrical nozzles with diameters (mm) of 23 (curve 1), 15 (curve 2), 11 (curve 3), respectively at water pressures P_0 = 1.6 MPa

Rys. 5. Rozkład prędkości osiowej (U_m) na długości zalewanego strumienia (l) dla dysz stożkowo-cylindrycznych o średnicach (mm) odpowiednio 23 (krzywa 1), 15 (krzywa 2), 11 (krzywa 3), przy ciśnieniu wody P_0 = 1,6 MPa

tubes, the set pressure on the nozzle was set and measurements were taken.

As a result of the experiments, the distribution of the dynamic pressure of the jet along its axis for nozzles of different diameters was obtained (Figure 5). After processing the experimental data and presenting them in the form of a dimensionless dependence, it was established that this dependence of the tested nozzles and pressures at a hydrostatic pressure of 1 m of water column is described by an equation similar to [61-69]

$$\frac{u_m}{u_o} = \frac{0,96}{0,29 + \frac{a_o l}{r_н}} \quad (6)$$

u_o – initial jet outflow velocity;
l – jet length;
$u_т$ – axis jet velocity;
$r_н$ – nozzle radius;
a_o – jet structure coefficient at low hydrostatic pressure (a0 = 0,068).

On the stand, the distribution of the flow velocity along the cross-sections of the jet from different nozzles in the pressure range of 0.4–1.6 MPa at a distance from 1 to 20 nozzle diameters was determined. Figure 6 shows velocity diagrams in different cross–sections of a jet with a 23 mm nozzle. In the boundary layer, the flow velocity is low and its value fluctuates greatly due to the turbulent exchange of the jet and the environment. Therefore, in order to identify the pattern of expansion of the jet of the hydromonitor, there was a The dependence of the flow velocity on the distance on the axis of the jet $r_{0,5m}$, at which the velocity of the jet is half of the axial velocity in the same section, is constructed in a dimensionless form u=0,5 $u_т$ (Figure 6 a, 6 b)

$$\frac{u}{u_m} = \exp\left[-\left(\frac{r_o}{r_{0.5u_m}}\right)^2 \ln 2\right] \quad (7)$$

Experimental data also show a linear expansion of the jet with an opening angle of α = 20°

$$r_{0.5u_m} / r_н = tg\frac{\alpha}{2} l / d_н \quad (8)$$

Study of the influence of the nozzle immersion depth on the parameters of the flooded jet. A special bench installation consisted of a chamber, which is a sealed pipe segment with a diameter of 400 mm and a length of 1500 mm, where the barrel of the hydraulic monitor is inserted. A measuring impulse tube of the pressure sensor is inserted from the other end of the chamber along the axis of the nozzle, which is secured and centered with a locking device.

The experiment starts with the installation and fixation of the nozzle and the receiving impulse tube at distances of 4, 10 and 20 nozzle diameters. When water is delivered to the chamber through the nozzle, the required value of hydrostatic pressure corresponding to the nozzle immersion is set in the

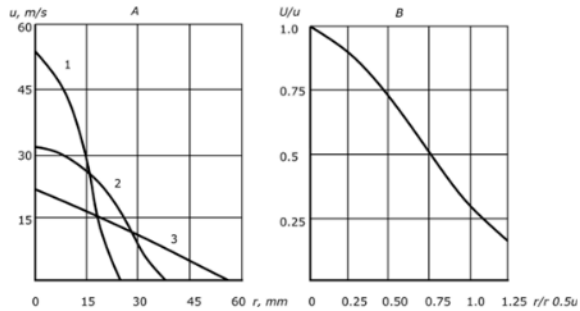

Fig. 6. Distribution of the flow velocity (u) of the flooded jet along the radius (r) of the cross–sections at distances from the nozzles (a) – 1 – 4 $d_н$; 2 – 10 dн; 3 – 20 d_0 (po = 1.6 MPa, dn = 23 mm); (b) – the same dependence in dimensionless form in the range of water pressure changes r_o = 0.4–1.6 MPa and nozzle diameters d_n = 11–23 mm

Rys. 6. Rozkład prędkości przepływu (u) zalanego strumienia wzdłuż promienia (r) przekrojów w odległościach od dysz (a) – 1 – 4 $d_н$; 2 – 10 $d_н$; 3 – 20 d_0 (po = 1,6 MPa, dn = 23 mm); (b) – ta sama zależność w postaci bezwymiarowej w zakresie zmian ciśnienia wody r_o = 0,4–1,6 MPa i średnic króćców d_n = 11–23 mm

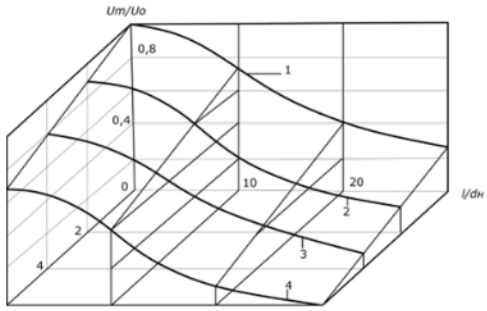

Fig. 7. Universal dimensionless dependence of the axial velocity of the flooded jet (U_m/U_0) of the hydromonitor nozzle on its length (l/dн) in sections 0, 1, 2, 3: 1 – at hydrostatic pressure p_r=1 meter of water column; 2 – p_r=20 meters of water column; 3 – p_r=40 meters of water column; 4 – p_r=60 meters of water column

Rys. 7. Uniwersalna bezwymiarowa zależność prędkości osiowej zalanego strumienia (U_m/U_0) dyszy hydromonitora od jej długości (l/dн) w przekrojach 0, 1, 2, 3: 1 – przy ciśnieniu hydrostatycznym p_r=1 metr słupa wody; 2 – p_r=20 metrów słupa wody; 3 – p_r=40 metrów słupa wody; 4 – p_r=60 metrów słupa wody

chamber using a relief valve and a pressure gauge. Then, the value of the axial dynamic pressure of the jet is measured.

The effect of hydrostatic pressure on the axial velocity increases with a decrease in the pressure at the nozzle outlet and practically does not depend on the nozzle diameters. The graph in Figure 7 shows that in the same jet cross–sections at a constant initial pressure with increasing hydrostatic pressure, the axial velocity decreases according to a linear law.

$$\frac{u_m}{u_0} = 1 - kp_0 \tag{9}$$

k – angular coefficient depending on initial pressure at nozzle inlet. For the conditions of the experiment k = 0,12–0,0054.

In the semi–empirical theory of the submerged jet [70, 73], the initial and boundary conditions of its flow are taken into account by the coefficient of the flow structure (a), empirically. Under our conditions, a dependence was obtained for differentinitial water pressures

$$a = \frac{1}{c - bp_0} \tag{10}$$

c – a constant equal to 16;
b – research coefficient.

Values of coefficient b are determined according to experimental data. For pressures (p0) 0.4; 0.8; 1.2; 1.6; 2.0 MPa; the b values are respectively 1.950; 1.471; 1.002; 0.560; 0.100.

The productivity of hydraulic fracturing per cycle was determined by dividing the volume of the product by the time of its formation. The specific water flow rate per 1 m³ of destroyed mineral was calculated as the ratio of water flow through the nozzle to the mineral volume destroyed during this cycle. Specific energy intensity was defined as the ratio of jet power to hydraulic fracture productivity per cycle.

Figure 8 shows the dynamics of the host rock destruction. The graph shows three stages in the destruction process. At the first stage, a narrow channel 1.1–1.7 m long is formed intensively, the extraction volume reaches 27%; in the second – the channel is expanded and deepened, the extraction volume increases to an average of 57%; At the third stage, the destruction productivity drops sharply, on average, the extraction volume is 16% and the channel length hardly increases, reaching about 2 m after 2–2.5 minutes.

As the face moves away from the nozzle, the fracture rate decreases (Figure 9, a), and the specific water flow rate increases (Figure 9, b). The distance from the face, at which the destruction of the mineral occurs, increases with an increase in the diameter of the nozzle. For example, with a water pressure of 1.5 MPa and nozzles of 11, 15, 23 mm, this distance is 1.2, respectively; 1,8; 2.05 m (Figure 10). As the water pressure increases, the fracture rate increases, and the specific water flow rate decreases and remains practically constant at a pressure of 1–1.5 MPa. The same happens when the diameter of the nozzle increases.

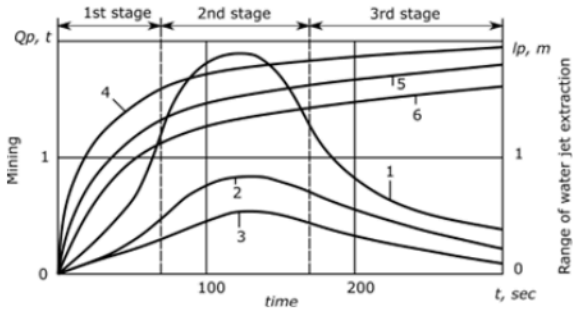

Fig. 8. Dynamics of hydraulic destruction of weakly cemented sand by a flooded jet from a single nozzle in time: 1, 2, 3 – Q_p=f(t); 4, 5, 6 – l p = f(t), respectively at p_0 = 1.5; 1.0; 0.5 MPa

Rys. 8. Dynamika niszczenia hydraulicznego piasku słabo zacementowanego przez zalany strumień z pojedynczej dyszy w czasie: 1, 2, 3 – Q_p=f(t); 4, 5, 6 – l p = f(t), odpowiednio przy p_0 = 1,5; 1,0; 0,5 MPa

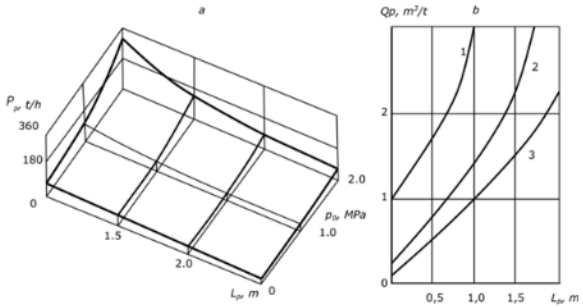

Fig. 9. Dependence of productivity (P_p) and specific flow rate (Q_p) and hydraulic fracture range or distance to face (L_p) on the value of pressure of pressure water (p_0): a – Pp =f(L_p); б – Q_p=f(L_p); 1, 2, 3 – for nozzle diameters of 11, 15 and 23 mm

Rys. 9. Zależność wydajności (P_p) i jednostkowego natężenia przepływu (Q_p) oraz zasięgu szczeliny hydraulicznej lub odległości od ściany (L_p) od wartości ciśnienia wody pod ciśnieniem (p_0): a – Pp =f(L_p); б – Q_p=f(L_p); 1, 2, 3 – dla dysz o średnicach 11, 15 i 23 mm

The productivity of destruction of a mineral flooded by a jet depending on (p_0 = 0,5–2 MPa, $d_н$=11–23 mm, L_p до 2 m) is described by empirical dependence (Figure 10).

One way to improve fracture performance is to use a special hydromonitor head, in which the jet of the side front nozzle rotates around the face perimeter. The head rotation is due to the jet reactive force. The jet of the central nozzle makes a cut in the host rock layer, and the rotating jet of the side nozzle, with one exposure plane, reflects the rock and widens the cut. As a result, a cavity will be formed, the size of which depends on the angle of the side nozzle inclination to the axis of the telescopic barrel and on the pressure of the pressurized water.

The fracture features and performance of the head are similar to those of a single nozzle. At the same time, the productivity is 2.5 times higher, and the minimum values of energy intensity and specific water consumption are 1.2–1.5 times lower. Increasing the side nozzle diameter, e.g. from 15 to 23 mm, gives a 50% increase in productivity at fracture. The optimal angle of the side nozzle is 50°.

The relationship between the main parameters of the flooded jet and the fracture is determined by the specific pressure needed for the destruction of a weakly cemented mineral with an adhesion coefficient of 0.030–0.045 MPa and an internal friction coefficient of 0.30–0.45. Table 1 shows the average values of the actual fracture range and specific pressure of the jet.

After analyzing the experimental data, generalized dependencies of fracture productivity (Pp) on jet power (N) were obtained

$$P_p = 2,0N^{0,933}, \text{ t/h} \quad (11)$$

Taking into account the well–known expression for the power of the jet, the formula will take the form

$$P_p = 165 d_н^3 p_0^{2,4} \cdot 10^{-4}, \text{ t/h} \quad (12)$$

One way to improve fracture performance is to use a hydraulic monitor with a telescopic barrel. By delivering the fracture mechanism to the face with a telescopic shaft, the fracture range can be increased by the shaft length (up to 10 m) and the jet kinetic energy can be used effectively due to the nozzle constantly approaching the developing face.

The host rock destruction in the flooded face was tested by delivering the head to the massif with a telescopic shaft. During the tests, when the head was delivered to the face, the water pressure was 1.5 MPa, and when it was delivered back, it was 0.5 MPa. The destruction was done by sector approaches by undercutting the layer along the sole, made of the loosest rock. The undercutting roadway diameter stabilized and averaged 1.6–1.8 m in all tests.

One of the important aspects for the technology of mineral extraction is the calculation of the angle between two undercutting workings, which prevents the creation of an undestroyed pillar. With a cutting roadway width of 1.8 m and a chamber radius of 8–9 m, the optimal angle between approaches is 15°.

2. Conclusion

The modeling studies determined the distribution of the hydromonitor flow speed across the jet cross-sections in the pressure range of 0.4–1.6 MPa at a distance of up to 20 nozzle diameters. A linear expansion of the jet with an opening an-

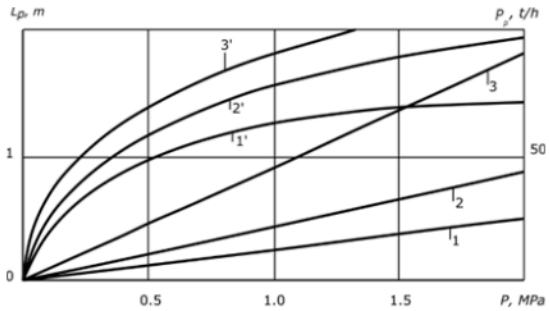

Fig. 10. Dependence of the average productivity (P_p) and fracture range (L_p) on water pressure (p_o): 1, 2, 3 – $P_p=f(p_o)$ d_H = 11, 15, 23 mm; 1', 2' ,3' – $l_p=f(p_o)$ at d_H = 11, 15, 23 mm

Rys. 10. Zależność średniej produktywności (P_p) i zasięgu pękania (L_p) od ciśnienia wody (p_o): 1, 2, 3 – $P_p=f(p_o)$ d_H = 11, 15, 23 mm; 1', 2',3' – $l_p=f(p_o)$ przy d_H = 11, 15, 23 mm

Tab. 1. Dependence of the fracture range of the host rock on the diameter of the nozzle

Tabela 1. Zależność zasięgu pękania skały macierzystej od średnicy króćca

Diameter nozzles, mm	Actual fracture range of the host rock, m	Distance from the nozzle, where the specific pressure jet is equal to 0.050 MPa
23	2,10	2,16
15	1,74	1,17
11	1,15	0,73

Tab. 2. Dependence of the Fracture Efficiency of the Host Rock on the Type destructive mechanism

Tab. 2. Zależność skuteczności pękania skały macierzystej od rodzaju mechanizmu niszczącego

Type of destruction mechanism	**Range destruction (limit), m**	**Average capacity, t/h**	**Pitoma vitrata waters, m³/t**	**Energy intensity, kWh/t**
Single nozzle diameter 11 мм 15 мм 23 мм	 1,15/(1,76) 1,74/(2,10) 2,10/(2,05)	 19,76/76,40 31,30/126,20 82,00/149,00	 0,76/0,197 1,10/0,28 0,72/0,50	 0,31/0,08 0,45/0,11 0,29/0,20
Hydromonitor head diameter 15 мм 23 мм	 2,0/(2,5) 2,6/(2,7)	 147,00/258 184,00/330	 0,603/0,340 0,680/0,375	 0,25/0,14 0,27/0,15
Hydromonitor head with telescopic barrel length 4.5 m, nozzle diameter 23 mm, feed rate 2.55 m/min	7,2/(7,3)	335/474	1,193/0,888	0,44/0,32

gle of 20° was established. In the same jet sections, the axial velocity decreases linearly with a coefficient of 0.12–0.0054, depending on the initial pressure at the nozzle outlet, as the hydrostatic pressure increases.

A flow structure coefficient of 0.068 was also found for different initial water pressures. The hydraulic destruction dynamics of rocks containing amber was studied, where three stages of the fracture process with different channel sizes and extraction volume intensities were identified respectively at 27%, 57% and 16%. The telescopic hydraulic monitor allows increasing the destruction range up to 10 m with stabilization of the undercutting roadway diameter of 1.6…1.8m.

Literatura – References

1. Dychkovskyi, R., Vladyko, O., Maltsev, D., & Cabana, E. C. (2018). Some aspects of the compatibility of mineral mining technologies. Rudarsko–Geološko–Naftni Zbornik, 33(4), 73–82. https://doi.org/10.17794/rgn.2018.4.7.
2. Perkovsky, E. E. (2017). Rovno Amber Caddisflies (Insecta, Trichoptera) from Different Localities, with Information about three New Sites. Vestnik Zoologii, 51(1), 15–22. https://doi.org/10.1515/vzoo–2017–0003.
3. Lustyuk M. G. Description of the technological scheme of the development of amber deposits / Bulletin of the NUVHP: Collection. of science works – Rivne, 2006. – No. 2 (34), part 1. – pp. 214–220.
4. Lustyuk M. G. Physico–technical basis of hydraulic extraction of lumpy minerals from placer deposits / Monograph – Rivne: Europ. Univ. PP DM – 2005. – 240 p.
5. Yussupov, Kh., Aben, Ye., Omirgali, A., & Rakhmanberdiyev, A. (2021). Analyzing a denitration process in the context of underground well uranium leaching. Mining of Mineral Deposits, 15(1), 127–133. https://doi.org/10.33271/mining15.01.127.
6. Begalinov, A., Khomiakov, V., Serdaliyev, Y., Iskakov, Y., & Zhanbolatov, A. (2020). Formulation of methods reducing landslide phenomena and the collapse of career slopes during open–pit mining. E3S Web of Conferences, 168, 00006. https://doi.org/10.1051/e3sconf/202016800006.
7. Shustov, O., Pavlychenko, A., Bondarenko, A., Bielov, O., Borysovska, O., & Abdiev, A. (2021). Substantiation into Parameters of Carbon Fuel Production Technology from Brown Coal. Materials Science Forum, (1045), 90–101. https://doi.org/10.4028/www.scientific.net/MSF.1045.90.
8. Zhanakova, R., Pankratenko, A., Almenov, T., & Bektur, B. (2020). Rational selection of the form of support for the formation of genetic composition of rocks in the conditions of the Beskempir field. News of the National Academy of Sciences of the Republic of Kazakhstan, (439), 106–113.
9. Begalinov, A., Almenov, T., Zhanakova, R., & Bektur, B. (2020). Analysis of the stress deformed state of rocks around the haulage roadway of the Beskempir field (Kazakhstan). Mining of Mineral Deposits, 14(3), 28–36. https://doi.org/10.33271/mining14.03.028.
10. Petlovanyi, M., Lozynskyi, V., Zubko, S., Saik, P., & Sai, K. (2019). The influence of geology and ore deposit occurrence conditions on dilution indicators of extracted reserves. Rudarsko Geolosko Naftni Zbornik, 34(1), 83–91. https://doi.org/10.17794/rgn.2019.1.8.
11. Telkov, S. A., Motovilov, I. Y., Barmenshinova, M. B., Medyanik, N. L., & Daruesh, G. S. (2019). Substantiation of Gravity Concentration to the Shalkiya Deposit Lead–Zinc Ore. Journal of Mining Science, 55(3), 430–436. https://doi.org/10.1134/s1062739119035769.
12. Korniienko, V., Malanchuk, Y., Zaiets, V., Semeniuk, V., Kucheruk, M. (2023). Research of the Dehydration Process of Amber–Containing Mining Mass. Inzynieria Mineralna, 1, 35–43. http://doi.org/10.29227/IM–2023–01–01.
13. Yulusov, S., Surkova, T. Y., Amanzholova, L. U., & Barmenshinova, M. B. (2018). On sorption of the rare–earth elements. Journal of Chemical Technology and Metallurgy, 53(1), 79–82.
14. Malanchuk, Z. V. Moshynskyi, Y. Malanchuk, V. Korniyenko, O. Vasylchuk, V. Zaiets, M. Kucheruk (2023). Impact by the operating and structural parameters of a screen on the technological parameters of vibratory basalt sieving. Mining of Mineral Deposits, 17(2), 35–43. https://doi.org/10.33271/mining17.02.035.
15. Begalinov, A., Shautenov, M., Almenov, T., Bektur, B., & Zhanakova, R. (2019). Prospects for the effective use of reagents based on sulfur compounds in the technology of extracting gold from resistant types of gold ore. Journal of Advanced Research in Dynamical and Control Systems, 11(8), 1791–1796.
16. Aben, E. K., Rustemov, S. T., Bakhmagambetova, G. B., & Akhmetkhanov, D. (2019). Enhancement of metal recovery by activation of leaching solution. Mining Informational and Analytical Bulletin, (12), 169–179. https://doi.org/10.25018/0236–1493–2019–12–0–169–179.
17. Remezova, O., Komsky M., Komliev O., Chukharev S., Vasylenko S. (2023). Study of Valuable Impurities of Ore–Forming Titanium Minerals in the Ukraine. Inzynieria Mineralna, 1, 189–194. http://doi.org/10.29227/IM–2023–01–24.
18. Bitimbaev, M. Z., Krupnik, L. A., Aben, E. K., & Aben, K. K. (2017). Adjustment of backfill composition for mineral mining under open pit bottom. Gornyi Zhurnal, (2), 57–61. https://doi.org/10.17580/gzh.2017.02.10.
19. Motovilov, I. Y., Telkov, S. A., Barmenshinova, M. B., & Nurmanova, A. N. (2019). Examination of the preliminary gravity dressing influence on the Shalkiya deposit complex ore. Non–Ferrous Metals, 47(2), 3–8. https://doi.org/10.17580/nfm.2019.02.01.
20. Arslanov, M. Z., Mustafin, S. A., Zeinullin, A. A., Kulpeshov, B. S., & Mustafin, T. S. (2020). Model for determining classification of filling materials hardening. News of National Academy of Sciences of the Republic of Kazakhstan, 5(443), 6–12. https://doi.org/10.32014/2020.2518–170x.98.
21. Mustakhimov, A., & Zeynullin, A. (2020). Scaled–up laboratory research into dry magnetic separation of the Zhezdinsky concentrating mill tailings in Kazakhstan. Mining of Mineral Deposits, 14(3), 71–77. https://doi.org/10.33271/mining14.03.071.

22. Pysmennyi, S., Fedko, M., Chukharev, S., Sakhno I., Moraru, R. and Panayotov, V. (2023). Enhancement of the rock mass quality in underground iron ore mining through application of resource–saving technologies. IOP Conf. Ser.: Earth Environ. Sci. 1156 012029. http://doi.org/10.1088/1755–1315/1156/1/012029

23. Malanchuk, Z.R., Korniyenko, V. Ya, Zaiets, V. V., Vasylchuk, O. Yu., Kucheruk, M. O. and Semeniuk, V. V. (2023). Study of hydroerosion process parameters of zeolite–smectite tuffs and underlying rock. IOP Conf. Ser.: Earth Environ. Sci. 1254 012051. https://doi.org/10.1088/1755–1315/1254/1/012051.

24. Malanchuk, Z.R., Khrystyuk, A.O., Stets, S.Ye. Semeniuk, V.V., Malanchuk, L.O. (2022). Substantiation of research results on energy efficiency of basalt crushing. Naukovyi Visnyk Natsionalnoho Hirnychoho Universytetu, (6), 41–46.https://doi.org/10.33271/nvngu/2022–6/041

25. Korniyenko, V.Ya, Vasylchuk, O.Yu, Zaiets, V.V., Semeniuk, V.V., Khrystyuk, A.O. and Malanchuk, Ye.Z. (2022). Research of amber extraction technology by vibroclassifier. IOP Conf. Ser.: Earth Environ. Sci. 1049 012027. https://doi.org/10.1088/1755–1315/1049/1/012027.

26. Malanchuk, Y., Moshynskyi, V., Khrystyuk, A., Malanchuk, Z., Korniienko, V., & Abdiev, A. (2022). Analysis of the regularities of basalt open–pit fissility for energy efficiency of ore preparation. Mining of Mineral Deposits, 16(1), 68–76. https://doi.org/10.33271/mining16.01.068.

27. Moshynskyi, V.S., Korniienko, V.Ya, Malanchuk, Ye.Z, Khrystyuk, A.O., Lozynskyi, V.H., Cabana, E.C. (2021). Simulation of amber extraction processes from sandy and clay rocks with stope filling. Naukovyi Visnyk Natsionalnoho Hirnychoho Universytetu, 6, 35–41. https://doi.org/10.33271/nvngu/2021–6/035.

28. Malanchuk, M., Zaiets, V., Tyhonchuk, L., Moshchych, S., Gayabazar G. and Dang T.(2021). Research of the properties of quarry tuff–stone for complex processing. E3S Web of Conferences. Volume 280 (2021) 01003 DOI:https://doi.org/10.1051/e3sconf/202128001003.

29. V. Korniyenko, V., Malanchuk Y., Khrystyuk, A., Kostrychenko V., Shampikova, A., Nogaeva K. and Kozhonov A. (2021). Modeling the distribution of rock mass and native copper output by size classes during crushing. E3S Web of Conferences. Volume 280 (2021) 01004 DOI:https://doi.org/10.1051/e3sconf/202128001004.

30. Dang, T., Malanchuk Z. and Zaiets T. (2021). Investigation of resistance and air leakage of auxiliary ventilation ducting in underground mine in Quangninh. E3S Web of Conferences. Volume 280 (2021) 08002 DOI:https://doi.org/10.1051/e3sconf/202128008002.

31. Nogaeva, K., Alpiyev, Y., Kozhonov, A., Korniyenko V. and Malanchuk Y. (2021). Technological basis of processing of serpentinite copper–gold ores in the Kyrgyz Republic. E3S Web of Conferences. Volume 280 (2021) 08005 DOI:https://doi.org/10.1051/e3sconf/202128008005.

32. Moshynskyi, V., Zhomyruk, R., Vasylchuk, O., Semeniuk, V., Okseniuk, R., Rysbekov K. and Yelemessov, K. (2021). Investigation of technogenic deposits of phosphogypsum dumps. E3S Web of Conferences. Volume 280 (2021) 08008 DOI:https://doi.org/10.1051/e3sconf/202128008008.

33. Malanchuk, Ye., Moshynskyi, V., Denisyuk, P., Malanchuk, Z., Khrystyuk, A., Korniienko, V., & Martyniuk, P. (2021). Regularities in the distribution of granulometric composition of tuff while crushing. Mining of Mineral Deposits, 15(1), 66–74. https://doi.org/10.33271/mining15.01.066.

34. Malanchuk, Ye., Korniienko, V., Malanchuk, L., Zaiets, V. (2020) Research into the moisture influence on physical–chemical tuff–stone characteristics in basalt quarries of the Rivne–Volyn region. E3S Web of Conferences. Volume 211 (2020) 01036 DOI:https://doi.org/10.1051/e3sconf/202020101036.

35. Small mining encyclopedia: in 3 volumes / edited by V. S. Biletskyi. — D.: Donbas, 2004. — T. 1: A — K. — 640 p. — ISBN 966–7804–14–3.

36. Svitlyi, Yu. G., Biletskyi V. S. (2009). Hydraulic transport (monograph). — Donetsk: Eastern Publishing House, Donetsk branch of the NTSh, "Editorial of the mining encyclopedia". 436 p. ISBN 978–966–317–038–1.

37. Korniyenko, V. , Nadutyi, V., Malanchuk, Y., Yeluzakh, M. (2020). Substantiating velocity of amber buoying to the surface of sludge–like rock mass. Mining of Mineral Deposits, 14(4), 90–96. DOI:https://doi.org/10.33271/mining14.04.090.

38. Malanchuk Z., Moshynskyi V.,Martyniuk P., Stets S., Galiyev D. (2020) Modelling hydraulic mixture movement along the extraction chamber bottom in case of hydraulic washout of the tuff–stone. E3S Web of Conferences. Volume 211 (2020) 01011 DOI:https://doi.org/10.1051/e3sconf/202020101011.

39. Malanchuk, Z., Moshynskyi, V., Malanchuk, Y.., Kor.niienko, V, Koziar, M. (2020). Results of Research into the Content of Rare Earth Materials in Man–Made Phosphogypsum Deposits. Key Engineering Materials, (844), 77–87. https://doi.org/10.4028/www.scientist.net/KEM.844.77.

40. Moshynskyi, V., Malanchuk, Z., Tsymbaliuk, V., Malanchuk, L., Zhomyruk, R., & Vasylchuk, O.(2020). Research into the process of storage and recycling technogenic phosphogypsum placers. Mining of Mineral Deposits, 14(2), 95–102. https://doi.org/10.33271/mining14.02.095.

41. Malanchuk Z., Korniyenko V., Malanchuk Ye., Khrystyuk A., Kozyar M. Identification of the process of hydromechanical extraction of amber. E3S Web of Conferences. Volume 166 (2020) 02008 DOI: https://doi.org/10.1051/e3sconf/202016602008.

42. Malanchuk, Z., Moshynskyi, V., Korniienko, V., Malanchuk, Y., Lozynskyi, V. Substantiating parameters of zeolite–smectite puff–stone washout and migration within an extraction chamber. Naukovyi Visnyk Natsionalnoho Hirnychoho Universytetu (2019). DOI: 10.29202/nvngu/2019–6/2.

43. Malanchuk, Z., Korniienko, V., Malanchuk, Y., Moshynskyi, V. Analyzing vibration effect on amber buoying up velocity.E3S Web of Conferences 123, 01018 (2019). Ukrainian School of Mining Engineering – 2019. DOI: 10.1051/e3sconf/201912301018.

44. Sai, K., Malanchuk, Z., Petlovanyi, M., Saik, P., Lozynskyi, V. Research of thermodynamic conditions for gas hydrates formation from methane in the coal mines. Solid State Phenomena (2019). DOI: 10.4028/www.scientific.net/SSP.291.155.

45. Malanchuk, Y., Korniienko, V., Moshynskyi, V., Soroka V., Khrystyuk, A., Malanchuk, Z. Regularities of hydromechanical amber extraction from sandy deposits. Mining of mineral deposits. – 2019. DOI: 10.33271/mining13.01.049.

46. Nadutyi, V., Korniyenko, V., Malanchuk, Z., Cholyshkina, O. Analytical presentation of the separation of dense suspensions for the extraction of amber. E3S Web of Conferences 109, 00059 (2019). Essays of Mining Science and Practice. DOI: 10.1051/e3sconf/20191090005.

47. Malanchuk, Z.V., Korniienko, V., Malanchuk, Ye., Soroka, V., Vasylchuk, O. (2018). Modeling the formation of high metal concentration zones in man–made deposits. Mining of Mineral Deposits, 12(2), 76–84. https://doi.org/10.15407/mining12.02.076.

48. Z. Malanchuk, Z., Moshynskyi, V., Malanchuk, Y., Korniienko, V. (2018). Physico–Mechanical and Chemical Characteristics of Amber. Non–Traditional Technologies in the Mining Industry. Trans Tech Publications Inc. Solid State Phenomena (Volume 277), pp. 80–89 doi: https://doi.org/10.4028/www.scientific.net/SSP.277.

49. Lozynskyi V., Saik P., Petlovanyi M., Malanchuk Z., Malanchuk Y. (2018). Substantiation into Mass and Heat Balance for Underground Coal Gasification in Faulting Zones. Inzynieria Mineralna. Journal of the Polish Mineral Engineering Society. DOI: 10.29227/IM–2018–02–36

50. Malanchuk Y., Moshynskyi V., Korniienko V., Malanchuk Z. (2018). Modeling the process of hydromechanical amber extraction. E3S Web Conf. Volume 60, Ukrainian School of Mining Engineering. https://doi.org/10.1051/e3sconf/20186000005.

51. Dychkovskyi, R.O., Lozynskyi, V.H., Saik, P.B., Petlovanyi, M.V., Malanchuk, Ye.Z., Malanchuk Z.R. (2018). Modeling of the disjunctive geological fault influence on the exploitation wells stability during underground coal gasification. Journal Archives of Civil and Mechanical Engineering. – 18(4), pp. 1183–1197. https://doi.org/10.1016/j.acme.2018.01.012.

52. Khomenko, O.Ye., Sudakov, A.K., Malanchuk, Z.R., Malanchuk, Ye.Z. (2017). Principles of rock pressure energy usage during underground mining of deposits. Scientific Bulletin of National Mining University/ Scientific and technical journal. Dnipro. Ukraine, PP KF «Gerda». №2(158). pp. 34–43.ISSN 2071–2227 UDC 622.831.24.0010.

53. Malanchuk, Z. (2017). Examining features of the process of heavy metals distribution in technogenic placers at hydraulic mining / Z. Malanchuk, Ye. Malanchuk, V. Korniyenko, I. Ignatyuk // Eastern – European Journal of Enterprise Technologies. № 1(10). – p. 45–51. – Режим доступу: http://nbuv.gov.ua/UJRN/Vejpte_2017_1(10)__7.

54. Malanchuk, Z., Korniienko, V., Malanchuk, Y. (2018). Results Of Research Into Amber Mining By Hydromechanical Method. Mining Of Mineral Deposits. T: 11. Vol. 1. p. 93–99. DOI: 10.15407/mining11.01.093.

55. Naduty, V., Malanchuk, Z., Malanchuk, E., Korniienko, V. (2016). Research results proving the dependence of the copper concentrate amount recovered from basalt raw material on the electric separator field intensity.Eastern – European Journal of Enterprise Technologies / PC «Technology Center», Kharkiv, Ukraine, Volume 5/5(83), p. 19–24. ISSN 1729–3774, UDC 622.277 DOI: 10.15587/1729–4061.2016.79524.

56. Malanchuk, Z., Malanchuk, Y., Khrystiuk, A. (2016). Mathematical Modeling Of Hydraulic Mining From Placer Deposits Of Minerals. Mining Of Mineral Deposits. T: 10. Vol. 2. p. 18–24. DOI: 10.15407/mining10.02.013.

57. Malanchuk, Y., Malanchuk, Z., Korniienko, V., Gromachenko, S. (2016). The Results Of Magnetic Separation Use In Ore Processing Of Metalliferous Raw Basalt Of Volyn Region. Mining Of Mineral Deposits. T: 10. Vol. 3. p. 77–83. DOI: 10.15407/mining10.03.077.

58. Malanchuk, Z., Korniienko, V., Malanchuk, E., Khrystiuk, A. (2016). Results of experimental studies of amber extraction by hydromechanical method in Ukraine. Eastern – European Journal of Enterprise Technologies / PC «Technology Center», Kharkiv, Ukraine, Vol.3/10(81), p. 24–28.(SCOPUS) ISSN 1729–3774, UDC 622.232.5:622.2 DOI: 10.15587/1729–4061.2016.72404.

59. Naduty, V., Malanchuk, Z., Malanchuk, E., Korniyenko, V. (2015). Modeling of vibro screening at fine classification of metallic basalt Text / Theoretical and Practical Solutions of Mineral Resources Mining, p. 441–443. doi: 10.1201/b19901–77.

60. Saik, P.B., Dychkovskyi, R.O., Lozynskyi, V.H., Malanchuk, Z.R., Malanchuk, Ye.Z. (2015). Revisiting the underground gasification of coal reserves from contiguous seams. New Developments in Mining Engineering: Theoretical and Practical Solutions of Mineral Resources Mining. №6. pp. 60–66. ISSN 2071–2227.

61. Fizyk, I., Prokhor, O., Kucheruk, M., Hrytsiuk, V. (2023). Ensuring environmental sustainability of forest ecosystems on disturbed lands with unauthorized amber mining. Key trends of integrated innovation–driven scientific and technological development of mining regions : multi–authored monograph. – Petroșani, Romania : UNIVERSITAS Publishing, p. 315–325. http://doi.org/10.31713/m1214.

62. Korniyenko, V.Ya. (2023). Research of deposits, their characteristics and features of amber occurence in amber bearing deposits of Ukraine and the world. Key trends of integrated innovation–driven scientific and technological development of mining regions : multi–authored monograph. Petroșani, Romani: UNIVERSITAS Publishing, p. 18–57. http://doi.org/10.31713/m1203.

63. Moshynskyi, V.S., Korniyenko V.Ya., Khrystyuk A.O., Solvar L.M. (2020). Research of energy effective parameters of the process of hydro mechanical extraction of amber from sandy deposits. Topical scientific researches into resource–saving technologies of mineral mining and processing. Multi–authored monograph. Sofia: Publishing House "St.Ivan Rilski", p. 24–38, 446 p. http://ep3.nuwm.edu.ua/17471.

64. Kryvoruchko, S.O. (2001). Products of the Rivne Region in Kyiv. S.O. Kryvoruchko: Khreshcha–tik newspaper.

65. Indutny, V.A. (1999). Stone colors of Ukraine: amber. V.A. Indutny. Geography and the basics of economics in school. No. 8. p. 26–31.

66. Kornienko, V. Ya. (2007). Analysis of modern technologies and the selection of equipment for the extraction of amber from sand deposits with the least technogenic and ecological impact on the environment / V. Ya. Kornienko // Bulletin of the NUVHP, Collection of Scientific Works, No. 2 (38). Rivne. p. 352–358.

67. Malanchuk, Z. R. (2009). Hydromining of minerals: scientific. study guide higher education closed. Z. R. Malanchuk, S. R. Boblyakh, E. Z. Malanchuk. National University of Water Management and Natural Resources Management. Rivne: NUVHP, 280 p.

68. The method of extraction of amber from the deposit. Patent of Ukraine (2000). No. 32201A dated 12/15. Bul. No. 7–II.

69. Arens, V.Zh. (1962). Investigation of parameters of hydromechanization during underground mining of ore deposits: author's review. thesis for obtaining sciences. candidate degree technical of Sciences / V.Zh. Ahrens. M. 137 p.

70. Kalabin, A.I. (1981). Extraction of useful minerals by underground leaching and other geotechnological methods / A.I. Kalabin. M.: Atomizdat, 1981. 302 p.

71. Kreiter V.M. (1960). Search and exploration of mineral deposits / V.M. Crater. – M.: Gosteoltekhizdat, t. I., 328 p.; 1961. Vol. II, 386 p.

72. Melnikov N.V. (1981). Mining engineers / N.V. Melnikov. M.: Nauka, 270 p.

73. Vlasyuk A.P. (1995). Numerical solution of one problem of dissolution and removal of formation salts from the base of hydraulic structures / A.P. Vlasyuk // Reports of the National Academy of Sciences of Ukraine. #8. p. 37–39.

74. Vabyshevich P.N. (1989). Adaptive nets of constant type in problems of mathematical physics / P.N. Vabyshevich // Journal. calculated mathematics and mathematics physicists. No. 6. pp. 902–914.

75. Burov A.P. (1952). Intructions for applying the classification of reserves of solid minerals. Al–Mazov rock deposits. A.P. Burov, G.I. Volarovich. M.: Gosgeolizdat, 40 p.

76. Vlasyuk A.P. (2005). Mathematical and computer modeling of the assessment of reserves of bulk minerals and the process of their extraction / A.P. Vlasyuk, M.G. Lustyuk. Abstracts of International Conference "Problems of decision making under uncertainties" (PDMU). Berdyansk, p. 107–109.

77. Burchakov A.S. (1985). Mine design / A.S. Burchakov, A.S. Malkin, M.I. Ustinov. M.: Nedra, 399 p.

78. Vabyshevich P.N. (1989). Adaptive nets of constant type in problems of mathematical physics / P.N. Vabyshevich. Journal. calculated mathematics and mathematics physicists. No. 6. p. 902–914.

Modelowanie wpływu hydraulicznego pękania skał bursztynośnych przez zalewany strumień w komorze erozji na wydajność górnictwa

W artykule omówiono koncepcję rozwoju społeczno-gospodarczego i strategicznego obwodu rówieńskiego (Ukraina), w szczególności poszukiwania, badania i przemysłowej eksploatacji strategicznych zasobów mineralnych. Koncepcja zakłada zastosowanie energooszczędnych technologii wydobycia surowca, zwłaszcza ze złóż bursztynu. Autorzy zwracają uwagę, że konwencjonalne metody wydobywania bursztynu są szkodliwe dla środowiska i sugerują stosowanie metod skomplikowanych, takich jak technologie mechaniczne i hydrauliczne.

W artykule podjęto problematykę wyzwań związanych z wdrażaniem metod geotechnologicznych w przedsiębiorstwach górniczych oraz dokonano oceny ich złożoności w nauce i praktyce górniczej. Prowadzono badania naukowe w tym zakresie. Kompleksowe badania metod pobierania próbek i wydobywania bursztynu są nadal istotne z punktu widzenia interesu narodowego.

Ponadto w artykule przedstawiono wyniki badań nad powstawaniem strumienia w monitorze hydraulicznym oraz zastosowania teleskopowego monitora hydraulicznego do poszerzania zasięgu fragmentacji skał, w tym analizę parametrów strumienia i dynamiki hydraulicznego kruszenia skał, m.in. skał bursztynonośnych. Wnioski dotyczą rozszerzalności liniowej strumienia, zmniejszania się prędkości osiowej wraz ze wzrostem ciśnienia hydrostatycznego oraz skuteczności hydromonitora teleskopowego w zwiększaniu zasięgu fragmentacji.

Słowa kluczowe: *bursztyn, hydromonitor, zanurzony strumień, zniszczenie, parametry*